Neutron diffraction, x-ray diffraction, and specific heat studies of orbital ordering in YVO_3

G. R. Blake and T. T. M. Palstra*
Solid State Chemistry Laboratory, Materials Science Centre, University of Groningen, Nijenborgh 4, 9747 AG Groningen, The Netherlands

Y. Ren
Argonne National Laboratory, 9700 South Cass Avenue, Argonne, Illinois 60439

A. A. Nugroho† and A. A. Menovsky
Van der Waals-Zeeman Institute, University of Amsterdam, Valckenierstraat 65, 1018 XE Amsterdam, The Netherlands

(Received 22 November 2001; published 25 April 2002)

Neutron diffraction, synchrotron x-ray diffraction, and specific heat studies have been carried out to investigate the nature of the ordered occupation of the vanadium *d* orbitals in perovskite YVO_3. Evidence has been found for a change in the type of orbital ordering at the 77-K phase transition in this material, manifested by a change in the type of Jahn-Teller distortion. This transition between orbital orderings is caused by an increase in octahedral tilting with decreasing temperature. The orbital ordering above 77 K is not destroyed at the magnetic ordering temperature of 116 K, but is present as far as a second structural phase transition at 200 K. The entropy changes at the onset of both spin and orbital ordering are much lower than the smallest semiclassical value of $R\ln 2$ J/(mole K).

DOI: 10.1103/PhysRevB.65.174112 PACS number(s): 61.10.Nz, 61.12.Ld, 61.50.Ks, 71.70.Ej

I. INTRODUCTION

The transition-metal perovskite oxides ABO_3 form the basis for many interesting physical phenomena such as high-T_C superconductivity, ferroelectricity, and colossal magnetoresistance. Despite these materials being the subject of intense study, in many cases their crystal structures have not been investigated in detail. For insulating materials containing a *B* cation with orbital degeneracy such as Ti^{3+}, V^{3+}, Mn^{3+}, and Ni^{3+}, long-range ordering of the occupied *d* orbitals is expected to take place below a transition temperature and will be accompanied by a Jahn-Teller (JT) distortion. There are very few undoped perovskite oxides for which JT distortions have been recognized.[1–5] However, orbital ordering can have profound and hitherto unrecognized effects on physical properties, such as the insulator-metal transition and charge order in doped $La_{1-x}M_xMnO_3$.[6,7]

We report here on the orbital ordering in YVO_3. The orbital ordering of t_{2g} electron systems is reflected structurally to a lesser extent than that of e_g systems, but can still have a dramatic influence on the physical properties. We show, using a combination of neutron-diffraction, synchrotron x-ray-diffraction, and specific-heat measurements, that the occupation of the t_{2g} orbitals in YVO_3 orders at 200 K; contrary to previous assumptions, this occurs far above the antiferromagnetic (AFM) ordering temperature $T_N=116$ K. Moreover, there is a change in symmetry of the orbital ordering at $T_S=77$ K. This is induced by an increased tilting of the octahedra with decreasing temperature, and it changes the easy axis of the V^{3+} d^2 $S=1$ spin, resulting in a magnetic structure transition and a reversal of the net ferromagnetic moment of the canted AFM state.

We have recently undertaken a detailed study of the unusual magnetic properties of YVO_3 single crystals.[8,9] YVO_3 adopts a distorted perovskite structure with the space group *Pbnm* at room temperature. It is an insulator, with the V^{3+} spins ($S=1$) ordering in AFM fashion below $T_N=116$ K, no change in the crystal structure being apparent. A reorientation of the ordered spins and a first-order structural phase transition involving a sudden change in the unit-cell volume takes place at $T_S=77$ K. Both above and below T_S a small canting angle of approximately 0.2° gives a net ferromagnetic moment that lies close to the *a* axis at all temperatures. When a magnetic field of less than 500 Oe is applied parallel to the *a* axis, reversible changes in the sign of the magnetization occur at both T_S and at $T^*=95$ K. The gradual magnetization reversal at T^* is thought to result from a competition between the single-ion magnetic anisotropy and an opposing Dzyaloshinsky-Moriya interaction. The more sudden reversal at T_S is a consequence of the reorientation of the ordered spins, which is thought to be associated with a change in the ordering of the occupied V *d* orbitals. Evidence of orbital ordering below T_S is clearly provided by the presence of a JT-ordered state.[9] A tetragonal distortion of the octahedra, where the long and short V-O bond distances alternate along the [110] and $[1\bar{1}0]$ directions of the *ab* plane, causes a splitting of the V t_{2g} orbitals into a doublet of lower energy and a singlet of higher energy. The doublet contains the *xy* orbital, which is always occupied, and either the *zx* or *yz* orbital. This ordered, alternating occupation of the V d_{zx} and d_{yz} orbitals between adjacent cations is shown schematically in Fig. 1. We believe that the change in magnetic structure from *G*-type below T_S to *C*-type above T_S (Ref. 10) is caused by a corresponding change from *C*- to *G*-type orbital ordering (Fig. 2). This statement is supported by the Goodenough-Kanamori rules,[11] band-structure calculations[12] and model Hartree-Fock calculations.[13] Experimentally, the only suggestion of *G*-type orbital ordering thus far has been provided by resonant x-ray scattering studies at the vana-

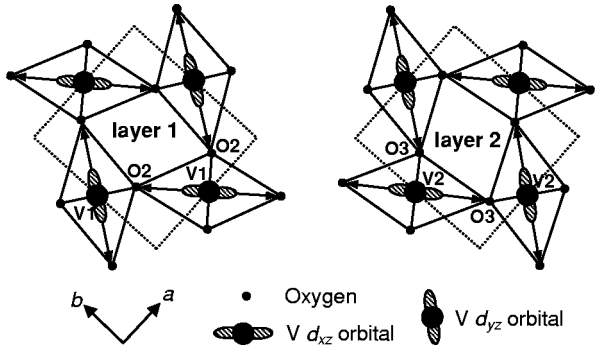

FIG. 1. Schematic picture of JT distortion in the ab plane of YVO_3 below 200 K; the unit cell is marked with a dotted line. Occupied V d_{zx} and d_{yz} orbitals are shown (x, y, and z refer to nominal cubic perovskite axes); d_{xy} orbitals are always occupied. There are two possible arrangements of alternating long (marked with arrows) and short V-O bonds, forming layers 1 and 2. Labeled atoms refer to those in the tables and text.

dium main K edge,[14] although there is still significant debate about the sensitivity to orbital ordering of this type of experiments.[15–17] In terms of the crystal structure, G-type orbital ordering is incompatible with $Pbnm$ symmetry, since two crystallographically distinct JT-distorted ab planes are required, with ''out-of-phase'' bonding arrangements; in $Pbnm$ all ab planes are rendered equivalent by the mirror planes at $z=1/4$ and 3/4, and the bonding arrangement is ''in phase.'' G-type orbital ordering is present in $LaVO_3$, which adopts the monoclinic space group $P2_1/a$ with β very close to 90°.[2] Here we provide crystallographic evidence of G-type orbital ordering above T_S, and our structural study also gives insight into the probable mechanism for the transition between orbital orderings.

II. EXPERIMENTAL METHODS

Polycrystalline samples of YVO_3 were prepared by the chemical reduction of YVO_4 powder. The YVO_4 powder was prepared by the high-temperature solid-state reaction of stoichiometric mixtures of predried Y_2O_3 (99.998%) and V_2O_5 (99.995%, metals basis). YVO_4 was reduced by annealing the powder in a flow of pure H_2 at 1000 °C. A single-crystalline boule of approximately 6 mm in diameter and 60–70 mm in length was grown by the travelling solvent floating zone method. The crystallinity of the boule was verified by Laue x-ray diffraction, and the elemental composition was checked by electron probe microanalysis, giving a resulting molar ratio of Y:V:O = 1.00:1.00:3.02. Time-of-flight neutron powder diffraction data were collected on the instrument POLARIS at the ISIS facility. Variable temperature data were collected by the backscattering detector bank over a d-spacing range $0.25 \leqslant d/\text{Å} \leqslant 3.0$, and by the low angle detector bank over the range $0.5 \leqslant d/\text{Å} \leqslant 8.1$, on samples of mass ~5 g (pulverized single crystals) contained in cylindrical vanadium cans inside a standard cryostat. An absorption correction was applied to all data sets at this stage using a routine incorporated in the Genie spectrum manipulation software.[18] The data were analyzed by the Rietveld method as implemented in the GSAS program suite.[19] The background levels of the neutron diffraction profiles were modeled using Chebyshev polynomials of the first kind (ten parameters). The peak shape of the profiles was described by a convolution of back-to-back exponentials and a pseudo-Voigt function (three parameters).

Synchrotron x-ray diffraction was performed on beamline ID11 at ESRF, on a small single-crystal fragment of approximate dimension 0.01 mm. The x-ray energy used was 42 keV, and temperature control was achieved by the use of cryogenic nitrogen and helium gas blowers; data were collected using a Bruker SMART 1500 charge-coupled device (CCD) camera. Integration of the frames was carried out using the SAINT+software,[20] incorporating the absorption correction program SADABS. Structural determination and refinement was carried out using the SHELXTL package.[21] Values for f′ and f″ at an x-ray energy of 42 keV were obtained using the data of Cromer and Liberman.[22]

Specific-heat measurements on both single crystal and pulverized crystal samples were carried out using a semiadiabatic heat pulse technique, with a Quantum Design MPMS system. Special care was taken to cool the sample slowly through the 77-K first-order phase transition, and the measurement was aborted if thermal contact to the sample was lost due to the discontinuous change in the lattice parameters.

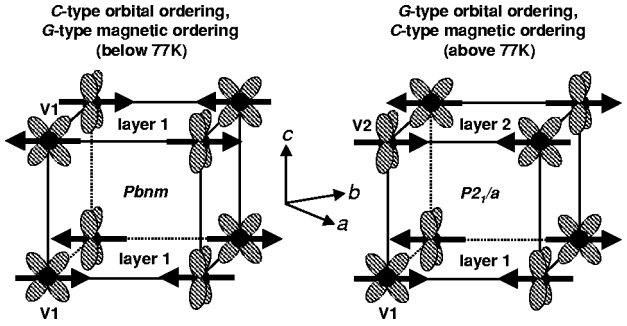

FIG. 2. Schematic representation of relationship between AFM ordering, orbital ordering and space group symmetry found in YVO_3. Occupied d_{zx} and d_{yz} orbitals are shown. Arrows represent AFM-ordered moments (arbitrary directions). The V-O bonding arrangement in successive layers (see Fig. 1) is either ''in phase'' ($Pbnm$) or ''out of phase'' ($P2_1/a$). Labeled atoms refer to those in the tables and text.

III. RESULTS

The starting model for Rietveld refinements using the neutron powder diffraction data was the 145-K structure of YVO_3 described by Nakotte *et al.*,[23] a $GdFeO_3$-type distorted perovskite with space group *Pbnm*. We retain this setting rather than using the standard $Pnma$ in order to be consistent with most of the previously published work on YVO_3 and related materials.[24] Since the neutron-scattering factor of vanadium is close to zero, isotropic temperature factors were fixed at reasonable values on the 4a vanadium site. Refinements at all temperatures proceeded smoothly. There is a clear phase transition between 65 and 80 K; at 65

K there are two short (1.991 Å) and one long (2.043 Å) V-O distances, the long and short bonds being arranged in an alternating pattern in the *ab* plane and indicating the presence of a JT distortion corresponding to *C*-type orbital ordering (Fig. 2). At $T=80$ K three inequivalent V-O distances ranging from 1.985 to 2.027 Å were obtained, the shortest distance being perpendicular to the *ab* plane and bonds within the plane differing by only 0.01 Å. To investigate the possibility of the symmetry being lower, as for $LaVO_3$, refinements were also carried out in the space group $P2_1/a$[24] using the $LaVO_3$ structure as a starting model, in which there are two inequivalent *ab* planes. Again, isotropic temperature factors were fixed to reasonable values on the $2b$ and $2c$ vanadium sites. No peaks were split or significantly broadened, since β remained close to 90°, but the fits to the data were marginally better than for *Pbnm* in the temperature range 80 K$\leqslant T\leqslant$180 K and marginally worse at 65, 240, and 295 K. The refined structures at 65, 240, and 295 K were essentially the same in both space groups, with β equal to 90° within a standard deviation. However, at intermediate temperatures there were significant structural differences between the refined *Pbnm* and $P2_1/a$ models, especially in terms of the V-O bond lengths. In the refined $P2_1/a$ structures these bond lengths were split into one long (2.041–2.060 Å) and two short (1.982–2.001 Å) distances, the long distance being in the *ab* plane. The bonding pattern was ''out of phase'' in successive planes, suggesting the presence of a *G*-type orbital ordering. The $P2_1/a$ space group is compatible with both types of JT distortion, and at 65 K the refined structure corresponded to *C*-type orbital ordering, with ''in-phase'' bonding patterns in successive planes. However, the difference in the quality of fit was in no case significant enough to conclude that the symmetry is ever lower than *Pbnm*.

The inconclusive structural refinement results from the powder diffraction study led us to continue our investigation using synchrotron x-ray single-crystal diffraction. It soon became apparent that many weak reflections violating *Pbnm* symmetry appeared on cooling through 200 K. For example, the intensity of one such forbidden reflection (401) is plotted as a function of temperature in Fig. 3. The inset to this figure shows the presence of some other reflections which violate the conditions for the *n*-glide plane, $(h0l), h+l=2n$. The $(0kl), k=2n$ condition still holds (not shown in this plot), and hence the *b* glide plane is retained. As expected, the highest symmetry space group compatible with the observed reflection conditions was number 14 in the International

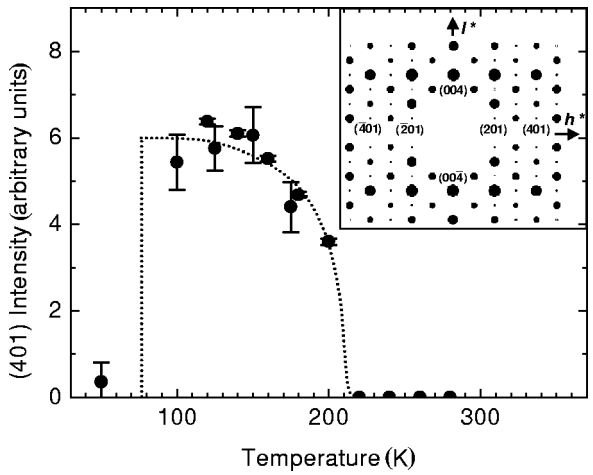

FIG. 3. Temperature dependence of the ''forbidden'' (401) reflection measured by synchrotron x-ray diffraction. Intensities with small error bars were integrated individually; intensities with large error bars were obtained from the automatic integration of an entire data file. The inset shows a section through reciprocal space obtained at 175 K where the (401) and other ''forbidden'' $(h0l)$, $h+l\neq 2n$ reflections are apparent; intensities of reflections are represented by sizes of circles.

tables; we have chosen the $P2_1/a$ setting rather than the standard $P2_1/c$ in order to retain the doubled perovskite *c* axis. The forbidden reflections could not be detected at 220 K but became easily visible at 200 K; their intensities increased on cooling before leveling off near 120 K and disappearing once more below 77 K. They provide definitive evidence of a phase transition with a lowering of the symmetry at approximately 200 K. The forbidden reflections are very weak compared to the strongest of the ''allowed'' *Pbnm* reflections, being of the order of 10^{-4} times as intense, and are therefore almost impossible to detect using a conventional laboratory x-ray source.

The data sets collected at 295, 225, and 50 K were consistent with the space group *Pbnm* and did not contain any extra reflections. The refinements proceeded smoothly and gave structures very close to those obtained from the neutron diffraction study at similar temperatures. A strong JT distortion corresponding to *C*-type orbital ordering was present in the 50 K structure. The data sets collected at 80, 100, 125, 150, and 175 K were consistent with the space group $P2_1/a$, and on refinement satisfactory values of *Rp*, *Rwp*, and χ^2 were obtained. However, on closer examination the observed

TABLE I. Lattice parameters for YVO_3.

T/K	Space group	a/Å	b/Å	c/Å	β/°	Volume / Å^3
295	$Pbnm$	5.27839(3)	5.60608(3)	7.57421(4)		224.129(1)
240	$Pbnm$	5.27574(3)	5.60679(3)	7.56714(4)		223.836(1)
180	$P2_1/a$	5.61126(3)	5.27474(4)	7.55316(4)	89.978(3)	223.558(1)
140	$P2_1/a$	5.61602(3)	5.27393(3)	7.54235(4)	89.973(3)	223.393(1)
100	$P2_1/a$	5.61940(3)	5.27272(3)	7.53499(4)	89.979(3)	223.258(1)
80	$P2_1/a$	5.62058(3)	5.27243(3)	7.53254(4)	89.977(3)	223.220(1)
65	$Pbnm$	5.28164(3)	5.58868(3)	7.55030(4)		222.865(1)

TABLE II. Atomic parameters for YVO_3 at 65 K. ($Rwp = 0.0142$, $\chi^2 = 1.836$).

Atom	Position	x	y	z	U_{11} or U_{iso}	U_{22}	U_{33}	U_{12}	U_{13}	U_{23}
Y	4*c*	0.97859(6)	0.42944(5)	3/4	0.0024(1)	0.0020(1)	0.0020(1)	0.0001(1)	0	0
V	4*a*	0	0	0	0.003					
O1	4*c*	0.88757(8)	0.96140(7)	1/4	0.0030(1)	0.0041(1)	0.0024(1)	0.0002(1)	0	0
O2	8*d*	0.18691(5)	0.29958(5)	0.05710(4)	0.0031(1)	0.0039(1)	0.0036(1)	-0.0005(1)	0.0007(1)	-0.0009(1)

intensities of many weak reflections were much greater than the calculated intensities, indicating the possibility of merohedral twinning. Furthermore, the expected JT distortion was absent, the pairs of V-O bonds in the *ab* planes being similar in length. It is well known that monoclinic structures that are metrically orthorhombic (that is, with $\beta \approx 90°$) are often pseudomerohedrally twinned on planes perpendicular to the *a* and *c* axes, where *b* is the unique axis.[25,26] For centrosymmetric structures such as YVO_3, the twinning does not produce extra reflections when $\beta = 90°$, but if the twin fractions are equal then the reflections (hkl), $(\bar{h}kl)$, $(h\bar{k}l)$ and $(hk\bar{l})$ become equivalent in intensity and the point group symmetry can appear to be raised from 2/*m* to *mmm*. Twinning of this type is reasonable if one imagines the unique *b* axis and either the *a* or *c* axis being initially established during crystal growth or during an orthorhombic-to-monoclinic phase transition. The third axis is then assigned to an arbitrarily left- or right-handed cell, which is equivalent to allocating the plus sign to the ''front'' or ''back'' of the plane containing the other two axes. There is no physical reason for one assignment to be favored over the other in a centrosymmetric structure, and therefore a pair of twin domains will often form when growth takes place simultaneously in opposite directions from a nucleation center, the twin boundary lying parallel to (100) or (001). Indeed, it may be expected that all centrosymmetric, monoclinic crystals with $\beta \approx 90°$ will display twinning involving domains of left- and right-handed unit cells. In the presence of an inversion center, changing the handedness of the unit cell is equivalent to performing a 180° rotation around the *a* or *c* axis, and the more conventional picture of uniform handedness can be retained for crystallographic purposes. Rotations of 180° around the *a* and *c* axes are equivalent by symmetry in the point group 2/*m*, so only two twin domains are present. This twin model was introduced for all data sets collected between 80 and 175 K, and the refinements were repeated, the twin fraction being refined. The average ratio of the two twin domains was 59–41 %, although refined values varied by up to 6% depending on the data set used. The resulting *Rwp* values were consistently lower; the 175-K data set was typical, with *Rwp* falling from 0.0875 to 0.0836. Further support for the twin model was provided by the fact that the *ab* planes now contained the expected alternating pattern of long and short V-O bonds in all of the refined structures between 80 and 175 K. The bonding pattern in successive planes was ''out of phase'' in all cases, characteristic of *G*-type orbital ordering.

The structures obtained from the synchrotron and neutron data refinements were very similar; the yttrium positions were determined rather more precisely from the synchrotron data, but the lattice parameters, oxygen coordinates, and thermal factors were better determined from the neutron data. In this case the two techniques are complementary; the synchrotron single crystal data are essential in order to detect the subtle lowering of the symmetry and unambiguously assign the correct space group, while the neutron powder data yield more accurate values for most structural parameters once the correct space group is known. The lattice parameters determined by neutron diffraction are given in Table I; atomic coordinates at representative temperatures of 65, 100, and 295 K are displayed in Tables II, III, and IV; and selected bond lengths and angles are listed in Table V. The observed, calculated, and difference neutron-diffraction patterns for a typical data set (100 K) are shown in Fig. 4.

The neutron-diffraction data collected from the POLARIS low-angle detector bank at $T \leqslant 100$ K showed peaks at high *d* spacings that could not be indexed using $Pbnm$ or $P2_1/a$ symmetry, but as expected, could be indexed in a *C*-type magnetic unit cell at 80 and 100 K and in a *G*-type magnetic unit cell at 65 K (Fig. 2); these data are very similar to those of Kawano *et al.*[10] Components of the ordered magnetic moments along each unit-cell axis were refined using the free-ion magnetic form factor of V^{3+},[27] the unit-cell parameters and all atomic parameters being fixed to the values obtained from the backscattering bank data. A purely antiferromagnetic system was assumed since the canting angle is small ($\sim 0.2°$).[9] At 65 K there are only two peaks with significant

TABLE III. Atomic parameters for YVO_3 at 100 K. ($Rwp = 0.0129$, $\chi^2 = 1.555$).

Atom	Position	x	y	z	U_{11} or U_{iso}	U_{22}	U_{33}	U_{12}	U_{13}	U_{23}
Y	4*e*	0.07051(6)	0.97967(6)	0.2496(2)	0.0028(1)	0.0029(1)	0.0023(1)	0.0000(1)	-0.0018(2)	-0.0007(3)
V1	2*c*	1/2	0	0	0.003					
V2	2*b*	0	1/2	1/2	0.003					
O1	4*e*	0.46064(7)	0.11131(7)	0.2501(4)	0.0043(1)	0.0032(1)	0.0026(1)	-0.0006(1)	-0.0011(5)	0.0005(4)
O2	4*e*	0.3088(2)	0.6947(2)	0.0561(4)	0.0045(3)	0.0033(3)	0.0034(4)	0.0002(2)	-0.0009(3)	0.0012(3)
O3	4*e*	0.7001(2)	0.3142(2)	0.5573(4)	0.0032(3)	0.0030(3)	0.0040(4)	-0.0012(2)	0.0008(3)	0.0002(3)

TABLE IV. Atomic parameters for YVO_3 at 295 K. ($Rwp = 0.0128$, $\chi^2 = 1.488$).

Atom	Position	x	y	z	U_{11} or U_{iso}	U_{22}	U_{33}	U_{12}	U_{13}	U_{23}
Y	4*c*	0.98071(7)	0.43061(6)	3/4	0.0058(1)	0.0050(1)	0.0049(1)	0.0005(1)	0	0
V	4*a*	0	0	0	0.005					
O1	4*c*	0.88885(9)	0.96031(9)	1/4	0.0053(2)	0.0073(2)	0.0040(1)	0.0013(1)	0	0
O2	8*d*	0.19084(6)	0.30408(6)	0.05640(4)	0.0054(1)	0.0064(1)	0.0063(1)	-0.0009(1)	0.0015(1)	-0.0019(1)

magnetic contributions; the (101) and (011) reflections could be perfectly fitted using a moment of $1.450(10)\mu_B$ parallel to *c*, which agrees with our previous result that the magnetic easy axis lies close to *c* below 77 K.[9] At 80 K there are four purely magnetic reflections, and the best fit was obtained by using two components [$0.895(13)\mu_B$ parallel to *b* and $0.649(15)\mu_B$ parallel to *c* in the *Pbnm* setting] giving a total moment of $1.106(10)\mu_B$. Our previous magnetization study suggested that the moments should be aligned with the easy axis close to *b*. The fit was only slightly worse on constraining the moment to lie in the *ab* plane, and given the limited number of magnetic reflections it is impossible to determine the directions of the moments for either magnetic structure unambiguously. Their magnitudes, however, are clearly much lower than expected for an $S=1$ system, a result which agrees well with the study of Kawano *et al.*[10]; one possible explanation could involve frustration of the superexchange interactions, and is discussed further below.

The specific-heat measurements provide strong evidence to support our conclusion that orbital ordering sets in at 200 K. Figure 5 shows the temperature dependence of the specific heat between 5 and 250 K. A discontinuity of $\Delta C = 3.53$ J/(mole K) occurs at 77 K, corresponding to the structural/orbital transition. This transition is clearly first or-

TABLE V. Selected bond distances (Å) and angles (degrees) for YVO_3.

	295 K (*Pbnm*)	240 K (*Pbnm*)	180 K ($P2_1/a$)	140 K ($P2_1/a$)	100 K ($P2_1/a$)	80 K ($P2_1/a$)	65 K (*Pbnm*)
Y-O1	2.2395(6)	2.2401(5)	2.2408(5)	2.2433(5)	2.2433(5)	2.2445(5)	2.2446(5)
Y-O1	2.2971(6)	2.2960(5)	2.2967(5)	2.2971(5)	2.2996(5)	2.3001(5)	2.2958(5)
Y-O2	2.2765(4)×2	2.2749(4)×2	2.267(2)	2.267(2)	2.266(2)	2.266(2)	2.2758(3)×2
Y-O2	2.4945(4)×2	2.4910(4)×2	2.487(2)	2.487(2)	2.485(3)	2.484(3)	2.4764(4)×2
Y-O2	2.6681(4)×2	2.6668(4)×2	2.656(3)	2.652(3)	2.655(3)	2.657(3)	2.6671(3)×2
Y-O3			2.281(2)	2.278(2)	2.278(2)	2.278(2)	
Y-O3			2.492(2)	2.488(2)	2.487(2)	2.485(3)	
Y-O3			2.669(3)	2.668(3)	2.662(3)	2.661(3)	
V1-O1	1.9948(2)×2	1.9934(1)×2	1.997(3)×2	1.993(3)×2	1.986(3)×2	1.987(3)×2	1.9905(1)×2
V1-O2	2.0129(3)×2	2.0130(3)×2	1.987(1)×2	1.981(1)×2	1.981(1)×2	1.981(1)×2	1.9909(3)×2
V1-O2	2.0256(4)×2	2.0255(3)×2	2.052(1)×2	2.058(1)×2	2.060(1)×2	2.060(1)×2	2.0433(3)×2
V2-O1			1.983(3)×2	1.982(3)×2	1.985(3)×2	1.982(3)×2	
V2-O3			2.001(1)×2	1.998(1)×2	1.997(1)×2	1.997(1)×2	
V2-O3			2.041(1)×2	2.047(1)×2	2.048(1)×2	2.047(1)×2	
V1-O-V1(V2)	143.33(3)	143.25(2)	143.22(2)	143.18(2)	143.17(2)	143.19(2)	142.99(2)
V1-O2-V1	144.85(2)	144.79(2)	144.87(9)	144.98(9)	144.88(10)	144.87(11)	144.75(2)
V2-O3-V2			144.60(10)	144.46(10)	144.57(11)	144.65(11)	
O1-V1-O2	87.71(2)	87.70(2)	87.49(7)	87.31(7)	87.36(8)	87.41(8)	88.07(1)
O1-V1-O2	88.63(2)	88.64(1)	88.66(7)	88.74(7)	88.70(8)	88.65(8)	88.97(1)
O1-V1-O2	91.37(2)	91.36(2)	91.34(7)	91.26(7)	91.30(8)	91.35(8)	91.03(1)
O1-V1-O2	92.29(2)	92.30(2)	92.51(7)	92.69(7)	92.64(8)	92.59(8)	91.93(1)
O2-V1-O2	89.352(6)	89.325(5)	89.55(3)	89.53(3)	89.54(4)	89.53(4)	89.197(5)
O2-V1-O2	90.648(6)	90.675(5)	90.45(3)	90.47(3)	90.46(4)	90.47(4)	90.803(5)
O1-V2-O3			87.94(7)	88.03(7)	88.02(8)	87.97(8)	
O1-V2-O3			88.73(7)	88.65(7)	88.74(8)	88.75(8)	
O1-V2-O3			91.27(7)	91.35(7)	91.26(8)	91.25(8)	
O1-V2-O3			92.06(7)	91.97(7)	91.98(8)	92.03(8)	
O3-V2-O3			88.98(3)	88.89(3)	88.80(4)	88.78(4)	
O3-V2-O3			91.02(3)	91.11(3)	91.20(4)	91.22(4)	

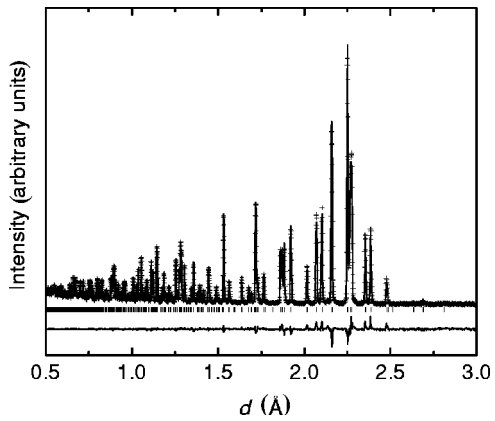

FIG. 4. Observed (crosses) calculated (solid line) and difference (lower line) neutron diffraction patterns for YVO_3 at 100 K. Tick marks indicate reflection positions. In this *d*-spacing range there are no magnetic peaks visible.

der, and is accompanied by a sudden change in the molar volume. Two lambda-shaped anomalies are obvious in Fig. 5, corresponding to the onset of magnetic ordering at 117 K and orbital ordering at 200 K. It is rather unclear how much entropy should be involved in these two transitions. The transition at T_N involves the antiferromagnetic ordering of a $S=1$ system, but the strong uniaxial anisotropy[9] will already remove much of the entropy above T_N. Therefore, we expect the magnetic ordering to involve entropy of the order of $S_{mag}=R\ln 2$ J/(mole K) rather than the $R\ln 3$ J/(mole K) expected for an isotropic spin system. The orbital ordering transition at 200 K involves the ordering of the d_{zx} and d_{yz} orbitals, while the d_{xy} orbitals are always occupied. Therefore, the onset of orbital ordering should yield a change in entropy of at least $R\ln 2$ J/(mole K). In order to evaluate these

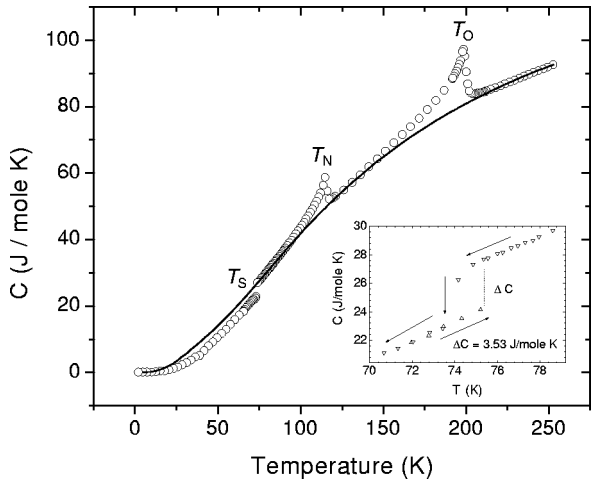

FIG. 5. Plot of specific heat vs temperature for an YVO_3 single crystal. Anomalies corresponding to the transition between orbital orderings at T_S, the onset of AFM ordering at T_N and the onset of orbital ordering at T_O, are indicated. The contribution of the crystal lattice to the specific heat, approximated by the sum of one Debye term and two Einstein terms, is shown as a solid line. The inset shows hysteresis on heating or cooling through the T_S first-order transition.

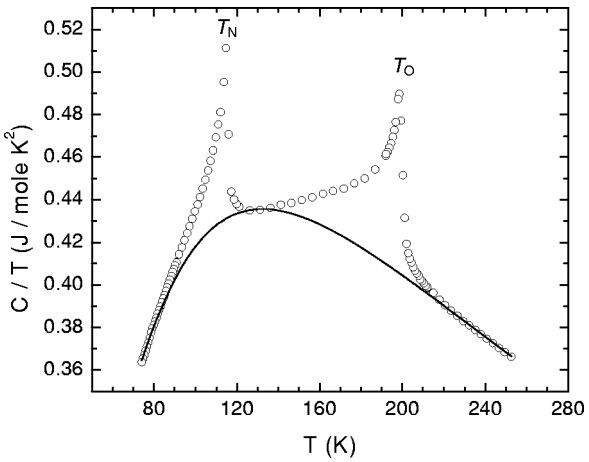

FIG. 6. Plot of C/T vs T for an YVO_3 single crystal, with the solid line indicating the lattice contribution.

entropy changes using the specific-heat data, the contribution of the crystal lattice should first be subtracted. Since there is no obvious reference compound without orbital or magnetic ordering, we choose to describe the lattice contribution using a combination of one Debye term and two Einstein terms. The Debye term originates from the low-energy acoustic modes, whereas the relatively heavy Y ion can give rise to high-frequency optical modes which are approximated by the Einstein terms. The lattice background is thus described by

$$C_{lat}=\alpha_D D(\theta_D/T)+\alpha_{E1}E(\theta_{E1}/T)+\alpha_{E2}E(\theta_{E2}/T),$$

where D and E are the Debye and Einstein functions, respectively. Good agreement with the experimental data over the entire temperature range was obtained using $\theta_D=200$ K, $\theta_{E1}=400$ K, $\theta_{E2}=900$ K, $\alpha_D=1.00$, $\alpha_{E1}=8.15$, and $\alpha_{E2}=4.05$ J/(mole K). The specific heat below 77 K is lower than the extrapolated curve, indicating a higher θ_D for the low-temperature phase. This is in agreement with the sudden lattice expansion observed on heating through the 77 K tran-

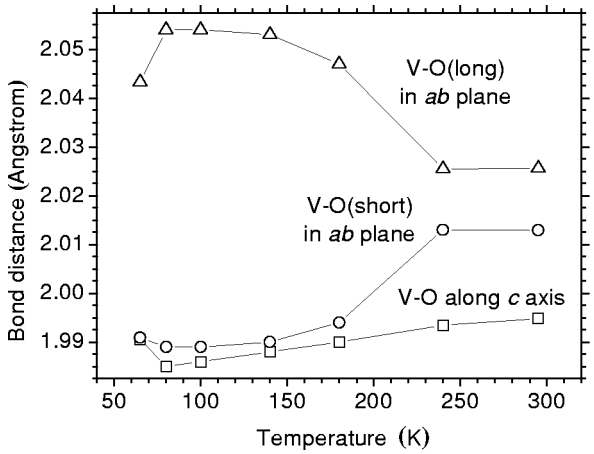

FIG. 7. Temperature dependence of V-O bond distances determined using neutron powder diffraction. For the $P2_1/a$ structures, the "long" and "short" distances [V1-O2 (long), V2-O3 (long) and V1-O2 (short), V2-O3 (short)] have each been averaged over the two ab planes. Typical errors are 0.001 Å.

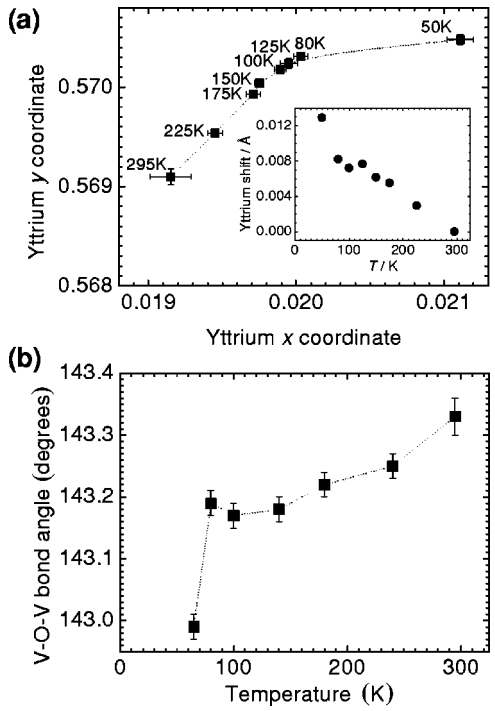

FIG. 8. (a) Variation of yttrium *x* and *y* coordinates with temperature; the inset shows the magnitude of the *Y* shift (zero point taken as the 295 K position). (b) Temperature dependence of the V-O1-V angle as an indicator of the degree of octahedral tilting along the *c* axis.

sition (Table I). The anomalies at T_N and T_O are plotted in Fig. 6 in the form C/T versus T. Taking the lattice contribution as a baseline, the areas under the peaks then give the entropy changes involved in the two phase transitions. The entropy change associated with the magnetic ordering at 117 K was estimated to be 0.81 J/(mole K), which is only 15% of the expected value of $R\ln 2$ J/(mole K). The orbital ordering entropy change was calculated to be 1.74 J/(mole K); while being twice the value of that at T_N, it is still only 30% of $R\ln 2$ J/(mole K), the minimum semi-classical value.

IV. DISCUSSION

The V-O bond lengths obtained from the neutron powder diffraction refinements in $P2_1/a$ are plotted as a function of temperature in Fig. 7. Those derived from the synchrotron data follow the same trend, but the values have larger standard deviations. At temperatures above the 200-K phase transition there are three unequal V-O bond distances, while below 200 K there is a clear JT distortion, the bonds being split into two short distances ($\sim$1.99 Å) and one long distance ($\sim$2.05 Å) in both orbitally ordered temperature regimes, the longer distance always being in the *ab* plane. The magnitude of the JT distortion is essentially constant from 200 down to 65 K, suggesting that the orbital degeneracy present at high temperatures is completely removed at 200 K. The difference between the longest and shortest bond lengths ($\sim$0.06 Å) is small compared to that in an e_g orbitally ordered system such as $LaMnO_3$ ($\sim$0.27 Å),[1] but similar to that present in $LaVO_3$ ($\sim$0.06 Å).[2] Differences in bond lengths of similar magnitude occur in $GdTiO_3$ and $YTiO_3$, which both appear to be orbitally ordered at room temperature;[3,4] they contain Ti^{3+} cations, where the t_{2g} orbitals are occupied by a single electron. Among the orthovanadates, the magnetic ordering temperature steadily decreases from 144 K for $LaVO_3$ (Ref. 28) to 101 K for $LuVO_3$,[29] as the lanthanide cation decreases in size from left to right across the series. This is due to an increase in the degree of octahedral tilting, which causes the vanadium $3d$ electrons to become more localized and the V-O-V superexchange interactions to become weaker. The general trend of the orbital ordering temperature in ABO_3 perovskites across the lanthanide series, as manifested by the onset of JT distortion, has been little investigated; among the orthovanadates the JT ordering temperature is only known for $LaVO_3$ [between 140 and 145 K (Ref. 2)] and now YVO_3 (200 K). This is perhaps due to the difficulty in recognizing the *G*-type orbital ordering present in these two materials (and which is probably a feature of all the orthovanadates from $LaVO_3$ to $DyVO_3$); it is incompatible with *Pbnm* symmetry, and can only be detected if a lowering of the symmetry to monoclinic is observed. In the case of YVO_3 the unit cell remains metrically orthorhombic, and the reflections violating *Pbnm* in diffraction experiments are so weak that single crystals and high intensity synchrotron radiation are required in order to detect the phase transition involved. For these *G*-type orbitally ordered materials, one would have to look specifically for the appearance of forbidden reflections with very low intensities, and these can easily be overlooked in a routine structural determination. An additional complication is the pseudomerohedral twinning inherent in perovskite single crystals that undergo an orthorhombic-to-monoclinic phase transition; this does not lead to the appearance of additional reflections and can be difficult to identify.

The yttrium position determined from the synchrotron refinements is plotted as a function of temperature in Fig. 8(a). The *z* coordinate has been neglected since it is fixed by symmetry for the *Pbnm* structures and deviates very little from 1/4 or 3/4 for the $P2_1/a$ structures. The yttrium cation does not remain in the same position relative to the fixed vanadium cations but moves steadily in the direction shown in Fig. 8(a) as the temperature is lowered to 80 K. Below the 77-K phase transition the shift appears to change direction, becoming close to [100]. The magnitude of the shift relative to the 295-K position [Fig. 8(a), inset] is of the order of 0.008 Å between 295 and 80 K, with a disproportionately large increase on cooling through the 77-K phase transition. The movement of the *A*-site cation is probably caused by an increase in the degree of octahedral tilting.[13] The bond angle V1-O1-V1 (and also V1-O1-V2 for the monoclinic structures), which characterizes the degree of tilting of octahedra along the *c* axis, is plotted as a function of temperature in Fig. 8(b). This angle decreases over the temperature range studied, and mirrors the trend of the yttrium site shift. The displacement of oxygen atoms from their ideal positions due to the octahedral tilting will tend to push the *A*-site cation in a given direction, as explained in detail by Mizokawa *et al.*[13] The driving force for this shift is the maximization of *A*-O

covalency (hybridization between the *A*-site cation *d* orbitals and the oxygen ion $2p$ orbitals); it is energetically favorable for the *A*-site cation to remain close to four nearest-neighbor oxygen ions, while little energy is lost in moving further away from the oxygen ions situated at a greater distance. This is the case for YVO_3 (Table V), showing that there are four Y-O distances of between 2.24 and 2.30 Å, the next shortest Y-O distance being ~2.49 Å. The *C*-type orbital ordering is stabilized by a high degree of octahedral tilting because two of the four closest oxygen ions, one in each of two successive *ab* planes, are moved in approximately the same direction by the corresponding JT distortion, allowing the *A*-site cation to be pushed in a given direction while retaining close contact with all four oxygen ions. However, when *G*-type orbital ordering is present, the oxygen ions in successive *ab* planes are ''out of phase'' with respect to each other and the *A*-site cation is pushed in two conflicting directions at once, decreasing the energy gain due to the *A*-O hybridization energy. It follows that *C*-type orbital ordering is predicted to be most stable for perovskites with a large degree of octahedral tilting, while *G*-type orbital ordering is more stable for lesser degrees of tilting, where the energy gain from the orbital ordering is greater than that from the *A*-O hybridization.[13] The type of AFM ordering is determined by the type of orbital ordering, if present, but the onset temperature of each is independent. In going from left to right across the lanthanide orthovanadate series, it has been reported that a change from ground-state *C*- to *G*-type AFM ordering takes place between $DyVO_3$ and $HoVO_3$ as the octahedral tilting increases;[29] this agrees with the above argument. A simultaneous transition from ground-state *G*- to *C*-type orbital ordering is almost certainly responsible for the crossover in AFM structures, but has not been investigated. The Y^{3+} cation is very similar in size to Ho^{3+}, and YVO_3 appears to be a unique material with octahedral tilting of a critical magnitude, at which both possible orbital ordering configurations are of similar energies. The slight increase in the degree of octahedral tilting with falling temperature causes a transition from *G*- to *C*-type orbital ordering on cooling through T_S. The rearrangement of the occupied orbitals in turn forces a change in the type of AFM configuration and in the direction of the easy axis, leading to a reversal of the net ferromagnetic moment.

There are two possible origins of the lower than expected entropy changes shown by the specific heat measurements. First, it is possible that the entropy involved in both the orbital ordering and magnetic ordering transitions is largely removed at high temperatures. The phase transitions would then only correspond to the ordering of orbitals or spins that are already strongly correlated. However, the origin of the strong deviations from mean-field theory in this almost isotropic material is not obvious. Second, it is possible that the small entropy changes are associated with frustration of the spin or orbital ground state. Khaliullin *et al.* recently claimed that spin and orbital interactions in the perovskite vanadates are highly frustrated.[30] They argued that fluctuations of the t_{2g} orbitals along the *c* axis trigger ferromagnetic interactions in this direction, yielding the *C*-type AFM structure adopted by $LaVO_3$ and by YVO_3 above 77 K; the JT effect only becomes dominant at low temperatures and can stabilize the *G*-type AFM phase. These fluctuations could also be responsible for the smaller than expected magnetic moment found in YVO_3 and also in the other rare-earth orthovanadates.[29] However, the assertions of Khaliullin *et al.* are based on a simplified structural model which neglects any influence of the degree of octahedral tilting; on the contrary, we argue above that this plays the most important role in determining the most stable magnetic structure, although orbital fluctuations may be responsible for the reduction of the ordered magnetic moment. In addition, our observation from diffraction data of a long-range JT distortion of essentially constant magnitude below 200 K implies that orbital ordering is effectively coherent on a length scale of 1000 Å or more. This does not exclude the possibility of short-range orbital fluctuations being present, but these fluctuations are not strong enough to destroy the long-range JT distortion and hence must be a relatively minor feature. The situation appears to be clearer in the $3d^1$ perovskite $LaTiO_3$, which is suspected to be an orbital liquid.[31] Neutron powder diffraction[32] and resonant x-ray scattering studies[33] have failed to reveal any evidence of orbital ordering, and this orbital liquid state is thought to be stabilized by quantum effects. It appears that the JT effect in $LaTiO_3$, although most likely present, is too weak to overcome these quantum effects, and hence orbital fluctuations dominate. In the absence of orbital ordering the *G*-type AFM structure is the most stable spin ground state. The proximity to the Mott transition seems to be an important factor regarding the presence of orbital fluctuations; $LaTiO_3$ has a band gap of only 0.2 eV, while that of $YTiO_3$ is approximately 1 eV.[34] $YTiO_3$ is reported to adopt a *C*-type orbital ordering,[33] which is consistent with the high degree of octahedral tilting in the structure (the Ti-O-Ti angle in the *c* direction is ~140°).[3] However, for a d^1 system with such pronounced octahedral tilting the ferromagnetic ground state is more stable than the *G*-type AFM state that would be expected from simple considerations of orbital symmetry in a perovskite with little octahedral tilting.[34] A similar suppression of the orbital ordering close to the Mott transition has also been observed in the doped manganites $La_{1-x}Ca_xMnO_3$; this appears to be a more important factor in inducing the ferromagnetic metallic state than a critical carrier density.[6]

V. CONCLUSIONS

Thus far, YVO_3 appears to be unique among perovskites in displaying a double magnetization reversal alongside two types of orbital and AFM ordering. However, the discussion above is most likely applicable to JT-distorted perovskites in general. The degree of octahedral tilting should be an important factor in all such perovskites in determining the most stable orbital ordering configuration and magnetic structure. It is worth studying related perovskites more closely to investigate whether the issues discussed here are in fact relevant to a broad range of materials, and to gain further insight into the interplay between octahedral tilting, orbital ordering and electronic properties.

ACKNOWLEDGMENTS

We thank R.I. Smith and G. Vaughan for experimental assistance at ISIS and ESRF, respectively. We are grateful to G.A. Sawatzky, D.I. Khomskii, A.A. Tsvetkov, A. Meetsma, and B.B. van Aken for useful discussions. This work was supported by the EU via the TMR Oxide Spin Electronics Network (OXSEN) and by the Netherlands Organization for Scientific Research (NWO).

*Corresponding author. Email address: Palstra@chem.rug.nl

†On leave from Jurusan Fisika, Institut Teknologi Bandung, Jl. Ganesha 10, Bandung 40132, Indonesia.

[1] J. Rodriguez-Carvajal, M. Hennion, F. Moussa, A. H. Moudden, L. Pinsard, and A. Revcolevschi, Phys. Rev. B **57**, R3189 (1998).

[2] P. Bordet, C. Chaillout, M. Marezio, Q. Huang, A. Santoro, S.-W. Cheong, H. Takagi, C. S. Oglesby, and B. Batlogg, J. Solid State Chem. **106**, 253 (1993).

[3] D. A. MacLean, H.-N. Ng, and J. E. Greedan, J. Solid State Chem. **30**, 35 (1979).

[4] J. R. Hester, K. Tomimoto, H. Noma, F. P. Okamura, and J. Akimitsu, Acta Crystallogr., Sect. B: Struct. Sci. **53**, 739 (1997).

[5] J. A. Alonso, M. J. Martínez-Lope, M. T. Casais, and M. T. Fernández-Díaz, Inorg. Chem. **39**, 917 (2000).

[6] B. B. van Aken, A. Meetsma, and T. T. M. Palstra (unpublished).

[7] Y. Endoh *et al.*, Phys. Rev. Lett. **82**, 4328 (1999).

[8] Y. Ren, T. T. M. Palstra, D. I. Khomskii, E. Pellegrin, A. A. Nugroho, A. A. Menovsky, and G. A. Sawatzky, Nature (London) **396**, 441 (1998).

[9] Y. Ren, T. T. M. Palstra, D. I. Khomskii, A. A. Nugroho, A. A. Menovsky, and G. A. Sawatzky, Phys. Rev. B **62**, 6577 (2000).

[10] H. Kawano, H. Yoshizawa, and Y. Ueda, J. Phys. Soc. Jpn. **63**, 2857 (1994).

[11] J. B. Goodenough, Prog. Solid State Chem. **5**, 145 (1963).

[12] H. Sawada and K. Terakura, Phys. Rev. B **58**, 6831 (1998).

[13] T. Mizokawa, D. I. Khomskii, and G. A. Sawatzky, Phys. Rev. B **60**, 7309 (1999).

[14] M. Noguchi, A. Nakazawa, S. Oka, T. Arima, Y. Wakabayashi, H. Nakao, and Y. Murakami, Phys. Rev. B **62**, R9271 (2000).

[15] M. Takahashi and J. I. Igarashi, Phys. Rev. B **64**, 075110 (2001).

[16] I. S. Elfimov, V. I. Anisimov, and G. A. Sawatzky, Phys. Rev. Lett. **82**, 4264 (1999).

[17] M. Benfatto, Y. Joly, and C. R. Natoli, Phys. Rev. Lett. **83**, 636 (1999).

[18] W. I. F. David, M. W. Johnson, K. J. Knowles, C. M. Moreton-Smith, G. D. Crosbie, E. P. Campbell, S. P. Graham, and J. S. Lyall, Open GENIE, Rutherford-Appleton Laboratory Report No. RAL 87-010, 1987 (unpublished).

[19] A. C. Larson and R. B. von Dreele, General Structure Analysis System (GSAS), Los Alamos National Laboratory Report No. LAUR 86-748, 1994 (unpublished).

[20] G. M. Sheldrick, SAINT+ NT, Version 6.02a, Bruker Analytical X-ray Instruments Inc., Madison, WI (2000).

[21] G. M. Sheldrick, SHELXTL, Version 5.1, Bruker Analytical X-ray Instruments Inc., Madison, WI (1998).

[22] D. T. Cromer and D. Liberman, J. Chem. Phys. **53**, 1891 (1970).

[23] H. Nakotte, L. Laughlin, H. Kawanaka, D. N. Argyriou, R. I. Sheldon, and Y. Nishihara, J. Appl. Phys. **85**, 4850 (1999).

[24] The unit cell of $a \approx 5.61$ Å, $b \approx 7.57$ Å, and $c \approx 5.28$ Å in the standard setting $Pnma$ is transformed to $a \approx 5.28$ Å, $b \approx 5.61$ Å, $c \approx 7.57$ Å in $Pbnm$; most of the listed citations use $Pbnm$, which we retain for consistency. We use $P2_1/a$ for the monoclinic phase ($a \approx 5.61$ Å, $b \approx 5.28$ Å, and $c \approx 7.57$ Å) instead of the standard setting $P2_1/c$ in order to retain the doubled perovskite c axis.

[25] G. M. Wolten and A. B. Chase, J. Chem. Phys. **41**, 2966 (1964).

[26] R. Herbst-Irmer and G. M. Sheldrick, Acta Crystallogr., Sect. B: Struct. Sci. **54**, 443 (1998).

[27] P. J. Brown, in *International Tables for Crystallography,* Vol. C., edited by A. J. C. Wilson (Kluwer, Dordrecht, 1995), p. 391.

[28] H. C. Nguyen and J. B. Goodenough, Phys. Rev. B **52**, 324 (1995).

[29] V. G. Zubkov, G. V. Bazuev, and G. P. Shveikin, Fiz. Tverd. Tela (Leningrad) **18**, 2002 (1976) [Sov. Phys. Solid State **18**, 1165 (1976)].

[30] G. Khaliullin, P. Horsch, and A. M. Oleś, Phys. Rev. Lett. **86**, 3879 (2001).

[31] G. Khaliullin and S. Maekawa, Phys. Rev. Lett. **85**, 3950 (2000).

[32] M. Eitel and J. E. Greedan, J. Less-Common Met. **116**, 95 (1986).

[33] B. Keimer, D. Casa, A. Ivanov, J. W. Lynn, M. v. Zimmermann, J. P. Hill, D. Gibbs, Y. Taguchi, and Y. Tokura, Phys. Rev. Lett. **85**, 3946 (2000).

[34] T. Mizokawa and A. Fujimori, Phys. Rev. B **54**, 5368 (1996).